THE JOURNAL OF PHYSICAL CHEMISTRY B

Article

pubs.acs.org/JPCB

Physicochemical and Functional Characterization of the Collagen–Polyvinylpyrrolidone Copolymer

Gerardo Leyva-Gómez,[†] Enrique Lima,[‡] Guillermo Krötzsch,[§] Rosario Pacheco-Marín,[∥] Nayeli Rodríguez-Fuentes,[⊥] David Quintanar-Guerrero,[#] and Edgar Krötzsch*[,†]

[†]Laboratory of Connective Tissue, Centro Nacional de Investigación y Atención de Quemados, Instituto Nacional de Rehabilitación, Mexico City, Mexico

[‡]Instituto de Investigaciones en Materiales, Universidad Nacional Autónoma de México, Circuito exterior s/n, Cd. Universitaria, Del. Coyoacán, C.P. 04510 México D. F., Mexico

[§]Instituto de Ciencias Físicas, Universidad Nacional Autónoma de México, Av. Universidad s/n, Col. Chamilpa, C.P. 62210, Cuernavaca City, Mexico

[∥]Laboratory of Molecular Biology, Instituto Nacional de Medicina Genómica, Periférico Sur 4124, Torre Zafiro II 5to piso, Col. Ex-Rancho de Anzaldo, Mexico City, Mexico

[⊥]Departamento de Materiales Metálicos y Cerámicos, Instituto de Investigaciones en Materiales, Universidad Nacional Autónoma de México, Circuito exterior s/n, Cd. Universitaria, Del. Coyoacán, C.P. 04510, México D. F., Mexico

[#]Laboratorio de Investigación y Posgrado en Tecnología Farmacéutica, Facultad de Estudios Superiores Cuautitlán, Universidad Nacional Autónoma de México, Av. 1° de Mayo s/n, Col. Sta. María las Torres, Cuautitlán Izcalli, Estado de México C.P. 54740, Mexico

ABSTRACT: Collagen–polyvinylpyrrolidone (C–PVP) is a copolymer that is generated from the γ irradiation of a mixture of type I collagen and low-molecular-weight PVP. It is characterized by immunomodulatory, fibrolytic, and antifibrotic properties. Here, we used various physicochemical and biological strategies to characterize the structure, biochemical susceptibility, as well as its effects on metabolic activity in fibroblasts. C–PVP contained 16 times more PVP than collagen, but only 55.8% of PVP was bonded. Nevertheless, the remaining PVP exerted strong structural activity due to the existence of weak bonds that provided shielding in the NMR spectra. On SEM and AFM, freeze-dried C–PVP appeared as a film that uniformly covered the collagen fibers. Size analysis revealed the presence of abundant PVP molecules in the solution of the copolymer with a unique dimension related to macromolecular combinations. Calorimetric analysis showed that the copolymer in solution exhibited structural changes at 110 °C, whereas the lyophilized form showed such changes at temperatures below 50 °C. The copolymer presented a rheopectic behavior, with a predominant effect of the collagen. C–PVP had biological effects on the expression of integrin α_2 and prolyl-hydroxylase but did not interact with cells through the collagen receptors because it did not inhibit or slow contraction.

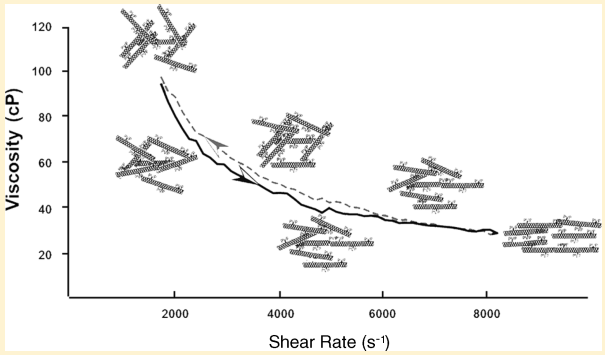

INTRODUCTION

Collagen–polyvinylpyrrolidone (C–PVP) is a compound derived from the γ irradiation of pepsinized porcine type I collagen fibers and low-molecular-weight (LMW) polyvinylpyrrolidone (PVP). The physicochemical and pharmacological properties of this copolymer are derived from its components. C–PVP exhibits immunomodulatory and tissue-regenerative properties, which have been evidenced in different pathologies in acute and chronic stages in various fields, including orthopedics and trauma,[1−4] vascular surgery,[5] gynecology and gastroenterology,[6−8] as well as dermatology and rheumatology.[9−15]

However, little is currently known about the structure of this copolymer. Polyacrylamide gel electrophoresis (PAGE) analyses have shown that C–PVP has a slight decrease versus collagen in the relative mobilities of the corresponding species to the α_1 (I) and α_2 (I) collagen chains.[16] High-performance liquid chromatography (HPLC) has shown that collagen has two species, whereas the copolymer and PVP have only one (unpublished observations). These findings, along with the observation that the biological activity of C–PVP differs from that of its individual components, suggest that these structural differences could determine the biological activity.[17]

Received: March 17, 2014
Revised: June 20, 2014
Published: July 22, 2014

   dx.doi.org/10.1021/jp502476x | J. Phys. Chem. B 2014, 118, 9272–9283

Table 1. Summary of the Samples and Assays with Which They Were Tested

sample	name	characteristic	assay[a]
polyvinylpyrrolidone K15	PVP	synthetic polymer	EC, SEM, AFM, NMR-MAS, DSC, particle size
irradiated polyvinylpyrrolidone K15	PVPirr	^{60}Co-irradiated synthetic polymer,10 KGy	NMR-MAS, DSC, particle size
type I collagen	collagen	biological polymer	SEM, AFM, NMR-MAS, DSC, digestion by MMP-1, rheology, particle size
collagen and polyvinylpyrrolidone	C+PVP	physical mixture (w/o irradiation)	AFM, NMR-MAS, DSC, rheology, particle size
collagen− polyvinylpyrrolidone	C−PVP	pharmaceutical grade copolymer (^{60}Co-irradiated, 10KGy)	EC, SEM, AFM, NMR-MAS, DSC, digestion by MMP-1, rheology, particle size, biological activity
collagen− polyvinylpyrrolidone w/ o excess polyvinylpyrrolidone	C−PVP/ −PVP	pharmaceutical grade copolymer (^{60}Co-irradiated, 10KGy), membrane filtration 100-kDa molecular cutoff	AFM, DSC, rheology, particle size

[a]EC = capillary electrophoresis, SEM = scanning electron microscopy, AFM = atomic force microscopy, NMR-MAS = nuclear magnetic resonance with magic angle spinning, DSC = differential scanning calorimetry, MMP-1 = matrix metalloproteinase 1.

The use of type I collagen and PVP as copolymer components is based primarily on their low immunogenicity and tolerance, respectively. Moreover, in vitro and in vivo assays have shown that C−PVP does not stimulate the proliferation of lymphocytes or cause DNA damage, nor does it induce the production of antibodies against porcine type I collagen or C−PVP. No evidence of renal or hepatic failure has been seen in patients receiving weekly doses of 0.2−1.0 mL of C−PVP for 1 year, either intradermally or intramuscularly.[18] On the basis of the above evidence, we sought to characterize the structure of the C−PVP copolymer through its physicochemical properties, biological susceptibility, and possible interaction with collagen-specific cell−surface receptors.

MATERIALS AND METHODS

Materials. Pepsinized porcine type I collagen (DSM Branch Pentapharm, Aesch, Switzerland) was dialyzed against 5 mM acetic acid (pH 4.3). PVP K-15 (8000 Da; ISP Investments, Inc., Wilmington, DE, U.S.A.) was dissolved in 5 mM acetic acid, and for some specified assays, it was irradiated at 10 kGy using a ^{60}Co pump (Instituto Nacional de Investigaciones Nucleares, Mexico City, Mexico). Both solutions were diluted in proportion to their content in C−PVP copolymer (Fibroquel, Aspid, SA de CV, Mexico City, Mexico), 8.33 and 133 mg/mL, respectively.

To assess whether PVP was affected by the irradiation used on the C−PVP copolymer, a fraction of the PVP solution was irradiated under the same conditions as the copolymer. To assess the proportion of PVP integrated into the copolymer, C−PVP was subjected to molecular filtration (Microcon 100 kDa, Millipore, Massachusetts, U.S.A.). For assays requiring materials in the solid state, samples were lyophilized (Freezone 6, Labconco, Missouri, U.S.A.). Table 1 summarizes the samples and assays with which they were tested.

Composition. *Chromatographic Characterization.* HPLC assays were performed in isopropanol−water−trifluoroacetic acid (80%: 19.99%: 0.01% v/v) as the mobile phase through a reverse-phase column (Chrompack P 300 RP, Chrompack, California, U.S.A.; 8 μm, 300 Å, and 150 × 4.6 mm ID). The analysis was run on a Varian chromatograph (Varian, California, U.S.A.) equipped with a Varian INERT 9012 pump and a Varian 9050 UV detector at 243 nm. The equipment was controlled with the Star Chromatography software (version 4.51). The injection volume was 60 μL, and the flow rate was 0.6 mL/min.

Electrophoretic Characterization. Capillary electrophoresis analysis was carried out on a ProteomeLab PA 800 (Beckman, California, U.S.A.) using the 32 Karat software. For electrophoretic separation of the samples, a negative capillary of 60 cm (50.3 cm to the detection window) × 50 μm ID was used. Detection was performed at 200 nm. Before each analysis, the capillary was washed for 5 min with running buffer (100 mM phosphate, pH 9.26). Before loading onto the capillary, the sample was diluted with ultrapure water (18 MΩ), injected hydrodynamically (5 s, 0.5 psi), and separated in running buffer at 30 °C and 10 kV.

Morphological Analysis. Micrographs were recorded using a Leica Stereoscan 440 scanning electron microscope (SEM) [Leica Microsystems, Bensheim, Germany]. Freeze-dried samples were fixed with 2.5% glutaraldehyde in phosphate buffer (PBS, pH 7.4, 0.1 M) for 1 h and washed with PBS and distilled water to prevent crystal formation. Subsequently, aluminum samples with carbon ribbon lacking a conductive material coating (gold, coal) were placed on a microscope slide.

The C−PVP copolymer was also analyzed by atomic force microscopy (AFM) on a JSPM 4210 microscope (JEOL, Tokyo, Japan); Mikromasch silicon cantilevers (NSC14) were used in measurements. A volume of 50 μL of the samples was diluted 1:100 and placed on a coverslip, and the samples were dried at room temperature with a relative humidity of 55%. After 7 days and with a final thickness of 5 μm approximately, the AFM analyses were performed. Every sample was placed on a copper bonding surface and analyzed in the contact mode to measure the topography of the sample in a scanned area close to 5 × 5 μm. The vibration frequency was in the range of 350 kHz. Images were acquired in the amplitude−height mode at room temperature.[19]

Structure. Liquid ^{1}H nuclear magnetic resonance (NMR) spectra were obtained in solutions diluted in D_2O using a Bruker Avance 400 spectrometer (Bruker, Billerica, Massachusetts, U.S.A.) at a frequency of 400.17 MHz. Samples were lyophilized prior to acquisition of ^{13}C NMR spectra with magic angle spinning (MAS NMR) in the solid state. Spectra were acquired on a Bruker Avance II 300 spectrometer (Bruker, Billerica, Massachusetts, U.S.A.) under cross-polarized conditions at a resonance frequency of 75.4 MHz and MAS of 5 kHz, using contact pulses of 100 μs and 1, 3, and 5 ms.[20]

The average particle size was determined by dynamic light scattering (DLS) on a Zetasizer (ZEN 3600 Nano - ZS, Malvern Instruments, Massachusetts, U.S.A.). The wavelength of the laser (He/Ne, 10 mW) was 633 nm. Measurements were obtained at an angle of 173° for 60 s at 25 °C. The sample concentration was adjusted to 830 μg/mL with a 5 mM acetic acid solution in all cases. Measurements were performed in quadruplicate.

Thermal Properties. Differential scanning calorimetry (DSC) was performed on a DSC Q10 (TA Instruments,

dx.doi.org/10.1021/jp502476x | J. Phys. Chem. B 2014, 118, 9272−9283

Delaware, U.S.A.) using airtight aluminum sample holders. The heating rate was 10 °C/min for samples in solution and 1 °C/min for lyophilized samples, with a range of 0−200 °C and a nitrogen flow of 50 mL/min. Each determination was performed in triplicate with only one scan. Enthalpy changes were determined from the experimental data.[21]

Susceptibility to Matrix Metalloproteinase (MMP)-1. Fibrillar collagens are biologically digested in two steps. First, the quaternary structure is denatured by interstitial collagenases, followed by digestion through gelatinases. Both enzyme groups belong to the family of MMPs.[22] An assay of enzymatic digestion of collagen and C−PVP by MMP-1 was conducted. Then, 400 μg of the collagen sample or an equivalent amount of C−PVP was incubated in the presence of 10 ng of MMP-1 (Sigma, Missouri, U.S.A.) in a tris-HCl buffer (pH 7.4) with $CaCl_2$, at 35 °C. Samples were incubated for different time periods (1−60 min). The reaction was interrupted by adding 20 μL of 0.1 M ethylenediaminetetraacetic acid (EDTA) to the reaction medium. Samples were centrifuged at 9000g at 4 °C for 10 min. Supernatants were tested in acrylamide gels at 10%. High-molecular-weight markers were run in the same gel to determine the size of the digested fragments.

Rheology and Frequency Spectra Analysis. Viscosity measurements were performed at 25 °C in 200 μL of sample, with the No. 1 needle of a Brookfield CAP 2000 viscometer (Brookfield, Massachusetts, U.S.A.). Each sample was analyzed in triplicate. The equipment was calibrated with standard solution No. CAP3L (Brookfield, Lot. No. 00601). The shear rate experiment was conducted from 1600 to 7999.98 s^{-1} (120−600 rpm) and vice versa at intervals of 1600 s^{-1}. All solutions were presheared at 1600 s^{-1} (120 rpm) for 5 min after loading into the concentric conical geometry. Each subsequent recording was taken after spinning for 20 s at each shear rate. Steady shear rate experiments were conducted at 2000 s^{-1} (150 rpm) using the same stabilization parameters. The total assay time was 2230 s.

The stiffness modulus was analyzed by the pseudo Wigner−Ville distribution (PWVD), which is the Fourier transform of the autocorrelation of the input signal. In this method, a signal $s(t)$ is transformed to the time−frequency domain. The distribution may be considered a spectral density function in its three-dimensional (3D) form. The calculation algorithm was implemented in the *Matematica 9* coding language.

The Wigner distribution (WDF) for a continuous signal is expressed as

$$w(t, \omega) = \int_{\infty}^{-\infty} s^*(t - \tau/2)s(t + \tau/2)e^{-i\omega\tau}\, d\tau \quad (1)$$

where w (t,ω) estimates the evolution in time of the power spectral density of the time signal $s(t)$. An analytical signal[23] was used as a simple approximation to mitigate the problems of aliasing

$$s(t) = s_r(t) + iH\{s_r(t)\} \quad (2)$$

The discrete version that was equivalent to eq 1 was used[24]

$$w(m\Delta t, k\Delta\omega) = 2\Delta t \sum_{n=0}^{2N-1} s[(m + n)\Delta t] \times s^*[(m - n)\Delta t]e^{-i\pi nk/N} \quad (3)$$

for N sample points at Δt intervals and for the frequency interval $\Delta\omega = \pi/(2N\Delta t)$.

A fast Fourier transform (FFT)-based algorithm was used. The representation of the algorithm was previously described by Shin and Jeon[24] in the Wahl and Bolton text[25]

$$w(m\Delta t, k\Delta\omega) = \mathrm{RE}\{2\Delta t\,\mathrm{FFT}[\mathrm{corr}(i)]\}$$

$$\text{where } 1 \le i \le N + 1$$

$$\mathrm{corr}(i) = \begin{cases} s(m + i - 1)s^*(m - i + 1) & m \ge i \\ 0 & m < i \end{cases}$$

$$\text{and } 2 \le i \le N \quad (4)$$

$$\mathrm{corr}(2N - i + 2) = \mathrm{corr}^*(i)$$

To minimize perturbations and negative values, a Gaussian window function was used of the form

$$G(p, q) = \frac{1}{2\pi jk\Delta t\Delta\omega} e^{-[(p^2/2j^2)+(q^2/2k^2)]} \quad (5)$$

for p and q integers in the ranges of $\pm 2j$ and $\pm 2k$, respectively, with the proviso that $j \cdot k \ge (N/\pi)$. Finally, convolving eqs 3 and 5, the PWVD was obtained

$$w'(l, m) = \frac{\Delta t\Delta\omega}{2\pi} \sum_{p=l-j}^{l+j} \sum_{q=m-k}^{m+k} w(p, q)G(p - l, q - m) \quad (6)$$

where $w'(l,m)$ is the smoothed function of eq 3.

In Vitro Assays on a Tridimensional Model. The 3D culture was prepared by mixing a 1.5× modified Dulbecco-Eagle culture medium (D-MEM; Gibco, Invitrogen, California, U.S.A.), supplemented with 10% fetal bovine serum (FBS), 2 mM glutamine, 100 U/mL penicillin, and 5 μg/mL streptomycin, with type I collagen at cold temperatures to a final concentration of 1 mg/mL and 2.5 × 10^4 cells/mL (human normal fibroblasts, fourth passage). The cell suspension was distributed in repeated 1.8 mL volumes in 24-well plates (Nunc, New York, U.S.A.). Immediately, 0.2 mL of C−PVP at 0.5, 1.0, and 3.0% (w/v) in D-MEM were added to the cultures. The negative control consisted of cultures treated with D-MEM. The positive control consisted of D-MEM with anti-β1 integrin antibody (1:500 dilution, only for contraction assays). Each assay was performed in triplicate.[26−28]

The cell suspension was allowed to gel. After 12 h of incubation, the contraction speed of the 3D systems was recorded every 3 h until 36 h had passed. Images of the cultures were acquired on a Gel-Doc Photodocumentation System (BIO-RAD, California, U.S.A.). The perimeter of the gel was defined, and the area was calculated from the images using the Axiovision software (Carl Zeiss, Göttingen, Germany), considering that at the start of incubation, the matrix occupied the entire area of the well (201.06 mm^2).

The integrin α_2 subunit is part of the heterodimer cellular receptor that recognizes type I collagen, among other components of the extracellular matrix (ECM). Prolyl hydroxylase is an enzyme synthesized by fibrobroblasts, involved in the post-translational modification of the endogenous collagen molecule. To evaluate the integrin α_2 and prolyl hydroxylase expressions, indirect semiquantitative immunofluorescence analyses were performed from 3D culture samples obtained at 12, 24, and 36 h, previously treated with C−PVP at 3.0% (w/v). Transverse cryosections (5 μm thick) of the frozen gels from different time points were made, and the

dx.doi.org/10.1021/jp502476x | J. Phys. Chem. B 2014, 118, 9272−9283

sections with antihuman mouse monoclonal antibodies were treated against α_2 integrin (mAb 1950, 1:100 dilution; Santa Cruz, California, U.S.A.) and prolyl hydroxylase (Clone 5B5, 1:50 dilution; Santa Cruz, California, U.S.A.). Nuclei were evidenced with diamidino-2-phenylindole (DAPI) and the antigens (α_2 subunit and prolyl hydroxylase) with fluorescein isothiocyanate (FITC). Slides were observed under a microscope (Axioimager Z1, Carl Zeiss, Gottingen, Germany) at 200×, with excitation light of 485 and 400 nm for FITC and DAPI, respectively. Images were acquired digitally and analyzed with Axiovision software to determine the density of the emitted fluorescence. To ensure that the fluorescence corresponded to a cell, only cases in which the label was found around a nucleus were considered.

Statistical Analysis. Statistical analysis of the immunofluorescence results was performed using the Mann−Whitney and Student's t tests. The contraction kinetics was analyzed using Tukey's test. Differences with p values of <0.05 were considered statistically significant.

RESULTS

On the basis of preliminary PAGE findings that the C−PVP copolymer had a different mobility pattern from collagen or the physical mixture (C+PVP),[16] an assay in which the copolymer was filtered through a membrane with a 100 kDa molecular cutoff was performed. After washing and analyzing the eluted (PVP) and retained copolymer (C−PVP/−PVP) fractions, it was found that the copolymer had a PVP-free fraction equivalent to 49.13 and 44.2% by HPLC and capillary electrophoresis, respectively (data not shown).

Morphology. In order to know the spatial distribution of the molecules at micro- and nanometers, we performed two complementary assays, SEM and AFM; both were very useful to identify the fibrillar pattern of collagen, the filmogen distribution of PVP, and the consequential properties of the composite (C−PVP).

The morphologies of the freeze-dried copolymer and its precursors were characterized using SEM. PVP formed a film with small irregular deposits of amorphous particles of 0.1 μm and large aggregates of more than 5 μm (Figure 1a). Collagen showed a fibrillar pattern similar to that observed when in the tissue (Figure 1b and e). The fibers were not completely smooth but were rough, a characteristic that was derived from their "native" state. On the other hand, C+PVP and C−PVP showed a hybrid morphology, namely, they appeared as a series of fibers "bathed" with a homogeneous film that covered most of the interfibrillar spaces (Figure 1c and d, respectively). This result was especially evident when the images were obtained at higher magnification (Figure 1f). Nevertheless, despite the similarity in morphological appearance, γ irradiation caused the formation of fragmented fibers (Figure 1d).

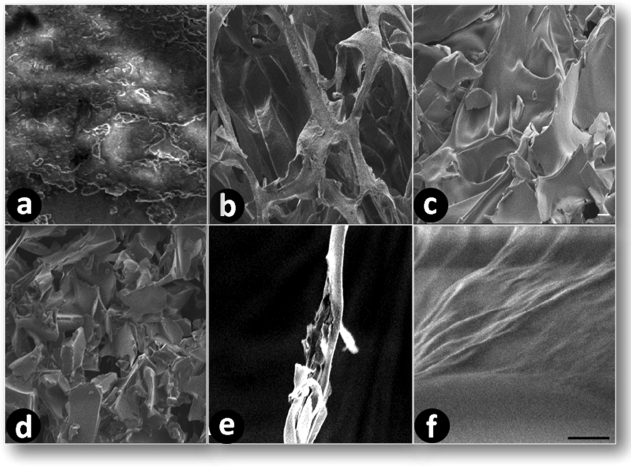

Figure 1. Photomicrographs obtained by SEM of freeze-dried (a) PVP, (b,e) collagen, (c) C+PVP, and (d,f) C−PVP. The scale bar is equivalent to 10 μm in a−d and 1 μm in e and f.

To characterize the irregularity of the copolymer fragmented fibers, C−PVP was subjected to AFM. C−PVP generally showed an irregular surface (Figure 2, left panel), corresponding to that observed by SEM (Figure 1f).[29−31] The line profiles calculated between points A and C showed variations in the surface material of up to 10 and 200 nm, respectively, indicating that the irradiation-induced cross-linking between collagen and PVP was accompanied by a change in texture. The AFM images (not shown) of the sample without irradiation (C+PVP) correspond to a smoother surface than those after irradiation. The wide range of diameters in collagen fibers and the induced cross-linking by irradiation are responsible for the surface modification. The cross-linking induced by irradiation occurred accompanied by the segmentation of collagen fibers, as supported by SEM and NMR results, and consequently, fibers were rearranged to result in a modification of the material texture.

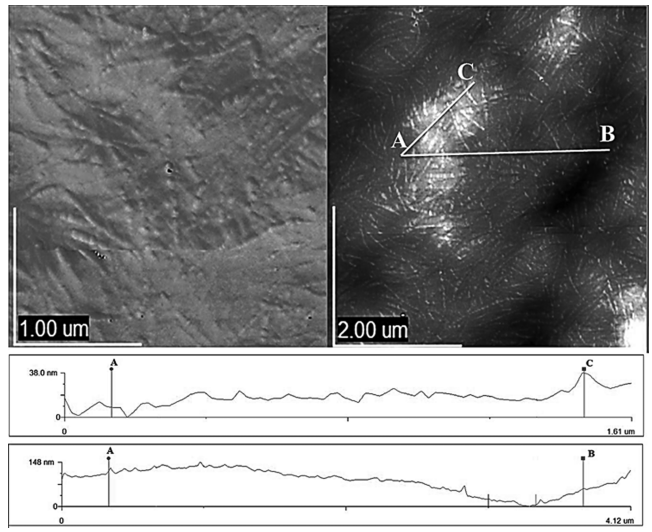

Figure 2. (Top) Images of the freeze-dried C−PVP copolymer obtained by AFM. The scale bars in lower left corners indicate the size in microns, 1.0 and 2.0 μm, respectively. (Bottom) Line profiles between points AC and AB.

Atomic Characterization. To elucidate whether collagen and PVP polymers were composed of parts that differed in their mobilities, ^{13}C NMR-MAS and ^{1}H NMR assays were performed. Figure 3A shows the ^{13}C NMR-MAS spectra of the copolymer in the solid state while varying the contact pulse. In the spectra of Figure 3A(a−c), the contact time varied from 5 ms to 100 μs, with no notable changes. Thus, it was concluded that collagen is a polymer that moves uniformly as it showed no significant change in the relationship of signal intensities. Moreover, variation in the pulse affected only the signal from the carbonyl group, which contains no protons.

dx.doi.org/10.1021/jp502476x | J. Phys. Chem. B 2014, 118, 9272−9283

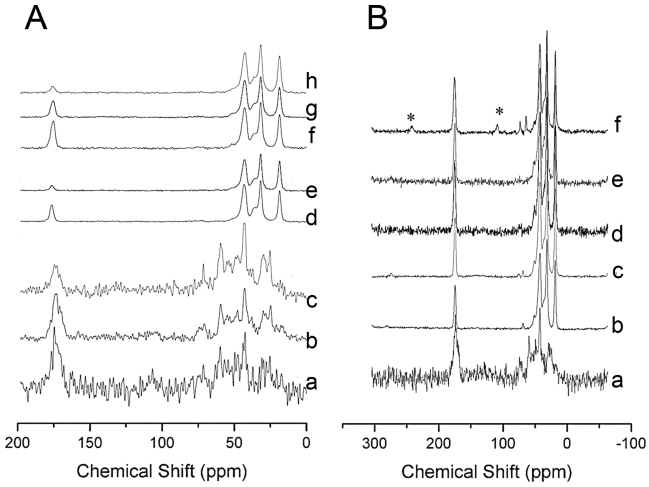

Figure 3. (A) ^{13}C MAS NMR spectra of freeze-dried samples under study for different contact times, 5 ms (a,f), 1 ms (b, d, and g), and 100 μs (c, e, and h). (B) Spectra acquired with 5 ms of contact time for (a) collagen, (b) PVP, (c) PVPirr, (d) C+PVP, (e) C−PVP, and (f) C−PVP/−PVP. *Rotation bands (5 kHz).

Thus, only changes in the magnetization transfer were observed. The same was true for PVP and PVP irradiated (PVPirr) (Figure 3A, spectra d,e and f−h, respectively), as Dumitraşcu M et al. also reported for 360 kDa PVP.[32]

Figure 3B compares the spectra of the pure polymers of C+PVP and C−PVP. There was no evidence of any specific interaction between the carbons of collagen and PVP. The spectrum for collagen showed typical signals at 172 ppm and in the window of 20−75 ppm [Figure 3B(a)]. These signals were due to carbonyl groups and aliphatic carbons, respectively,[33] which are amino acid residues that form part of the collagen structure. The spectra of PVP and PVPirr also exhibited signals due to carbonyl groups and aliphatic carbons [Figures 3B(b,c)], such that the spectra of C+PVP and C−PVP were very similar to the spectrum of PVP [Figures 3B, spectra d and e, respectively].

The spectrum of C−PVP/−PVP [Figure 3B(f)] was also very similar to PVP, but in this case, some signals (at 73 and 62 ppm) typical of collagen could be seen. However, the position and width of these peaks were very similar to those of pure collagen. Thus, it cannot be concluded that there was an interaction via the aliphatic carbons; interaction through other carbons was difficult to elucidate because of the intense bands of PVP.

Figure 4A compares the ^{1}H NMR spectra acquired in liquid samples for collagen, PVP, PVPirr, C+PVP, and C−PVP. In Figure 4A(a), two peaks between 2.9 and 2.7 ppm were observed, corresponding to hydrogens bound to the α carbons of proline, glycine, and so forth,[34,35] typical of the most abundant amino acid residues in collagen. At a higher field (2.1 ppm), shielded hydrogens were identified, such as those bonded to the carbons of alanine. Peaks corresponding to OH and NH groups were not observed because the hydrogens of these groups are easily interchangeable in the solvent used (D_2O).

The spectrum of PVP was completely resolved and is shown in Figure 4A(b). It was assigned displacement values corresponding to the monomeric structure of PVP depicted in Figure 4B. Peaks near 1.4 ppm can be attributed to the terminal methyl groups ($-CH_3$) of the polymer chains.

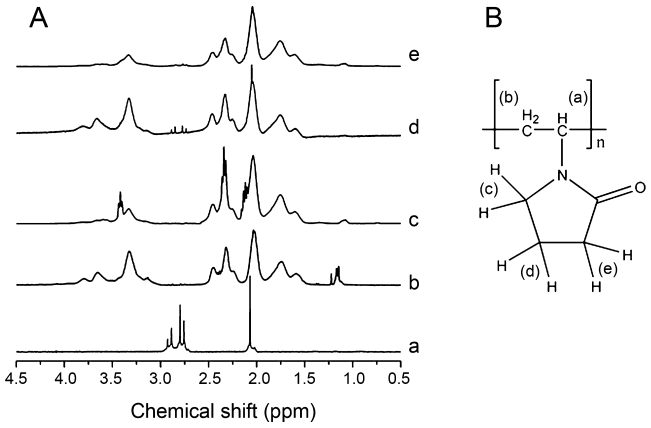

Figure 4. (A) ^{1}H NMR spectrum of samples under study diluted in D_2O. (a) Collagen, (b) PVP, (c) PVPirr, (d) C+PVP, and (e) C−PVP. (B) Structure of PVP, with carbons labeled for assigning corresponding ^{1}H NMR signals.

However, the spectrum of PVP was changed as a result of γ irradiation [Figure 4A(c)]. The thin peaks attributed to the $-CH_3$ terminals appeared as a broad signal, which can be interpreted as a loss of mobility of these groups.[36] This effect was opposite to that observed in broad peaks attributed to the ring hydrogens, which showed additional thin and overlapping signals, which can be explained as the gain in mobility in these hydrogens (Table 2). Finally, the intensity of the methylene group ($-CH_2$) decreased significantly, suggesting that PVP depolymerization occurred due to γ irradiation.

Table 2. Assignment of the ^{1}H NMR Resonance Values for the PVP Diluted in D_2O

chemical shift (δ), ppm	types of hydrogen[a]
3.81−3.65	CH(b)
3.42−3.30	CH_2(c)
2.55−2.31	CH_2(e)
2.11−1.90	CH_2(d)
1.75−1.59	CH_2(a)

[a]According to the structure included in Figure 4B.

The C+PVP spectrum [Figure 4A(d)] was composed mainly of PVP signals, although it presented some differences compared to the pure polymer. In particular, the thin signals attributed to terminal $-CH_3$ in PVP disappeared when PVP was physically mixed with collagen, perhaps because PVP lost mobility due to its increased molecular mass. This result implies that there is an interaction between the two polymers;[37] otherwise, the NMR signals would have remained unchanged. The spectrum of C−PVP [Figure 4A(e)] showed some differences from the spectrum of the physical mixture. The thin peaks of collagen and signals from the $-CH_2$ groups of PVP were decreased significantly, consistent with the idea that irradiation decreases the degree of polymerization of PVP. As a result, the shorter chains of PVP would be able to intersect with collagen, resulting in a composite with very low mobility.

Irradiation produces morphological and structural changes in the C−PVP molecule; for that reason, the resulting particle size and the three most important distributions of molecular size in the range of 1−3000 nm were assessed (Table 3). The aggregate size reported as peak 3 was similar for C+PVP and C−PVP. Therefore, PVP noticeably altered the aggregation

dx.doi.org/10.1021/jp502476x | J. Phys. Chem. B 2014, 118, 9272−9283

Table 3. Aggregation Sizes Using DLS[a]

	peak 1		peak 2		peak 3	
sample	mean particle size (nm)	area (%)	mean particle size (nm)	area (%)	mean particle size (nm)	area (%)
collagen	16.6 ± 2.3	17.1 ± 1.5	56.4 ± 2.4	23.6 ± 20.6	2049.8 ± 1946	54.3 ± 27.6
PVP	5.5 ± 0.4	89.8 ± 4.0	182.8 ± 25.2	10.2 ± 4.0	0.0	0.0
PVPirr	5.4 ± 0.0	92.8 ± 0.6	17.9 ± 15.0	49.72 ± 32.2	149.8 ± 49.3	3.9 ± 1.6
C+PVP	5.4 ± 1.2	41.4 ± 13.7	31.0 ± 18.9	17.6 ± 10.8	955.4 ± 254.0	36.1 ± 3.3
C−PVP	6.1 ± 0.7	41.7 ± 5.0	36.9 ± 12.2	12.2 ± 3.7	912.1 ± 266.5	46.1 ± 7.5
C−PVP/−PVP	5.5 ± 0.1	49.1 ± 4.2	21.7 ± 1.2	12.9 ± 0.6	485.4 ± 26.6	38 ± 4.8

[a]Peak area = percentage of the area of the corresponding peak.

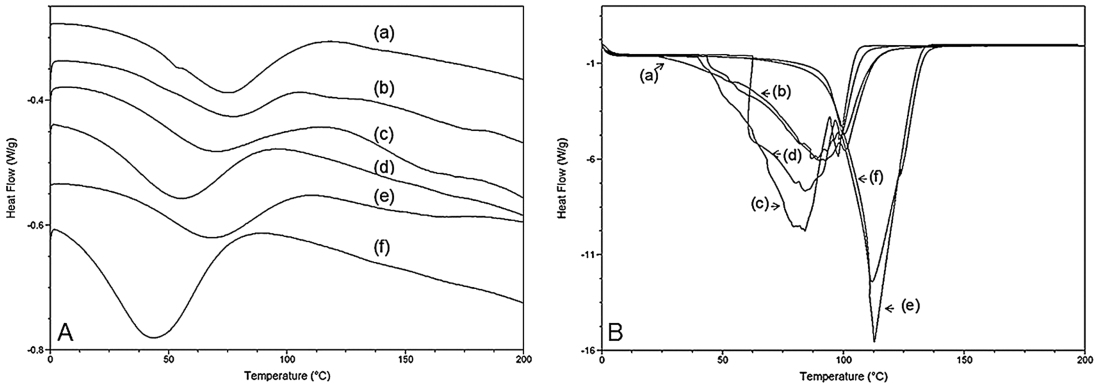

Figure 5. DSC thermograms of lyophilized samples (A) and thermograms of samples in solution (B). (a) PVP, (b) PVPirr, (c) collagen, (d) C+PVP, (e) C−PVP, and (f) C−PVP/−PVP.

state of the protein, probably via various types of interactions, such as temporary hydrogen bonds.[37] However, peak 3 for the C−PVP/−PVP sample showed a smaller aggregate size (485.4 ± 26.6 nm) compared to that for C+PVP and C−PVP, confirming that there is a direct relationship between the amount of PVP present and the aggregate size. The size of the largest peak of the copolymer decreased with a decrease in the presence of PVP. This result could be interpreted as indicating a change in the molecular association state in the absence of the free-aggregating component.

Thermal Properties. A key aspect of the copolymer is its thermal stability. The compound is made from "native" collagen, which is susceptible to denaturation at a temperature slightly above physiological.[38] Calorimetric assays were conducted using a DSC system, in which samples were evaluated in the solid (lyophilized) state and in solution.

Figure 5 shows the thermal behavior of the copolymer and its separate components. In the solid state, before and after irradiation, the PVP sample exhibited transition temperatures of 75.0 and 77.5 °C, respectively [Figure 5A(a,b)], corresponding to the glass transition temperature (T_g) and loss of water, respectively.[39−43] There was a significant decrease in the ΔH values from 162.1 to 126.9 J/g (Table 4). These values are related to the association of the material with water. A similar reduction was obtained for samples in solution [Figure 5B(a,b)]. The increase in T_g confirms the results of the structural characterization due to the irradiation process (Figure 3A(e), NMR analysis). PVP is a hygroscopic material; thus, a change in the heat capacity is affected by the presence of water vapor.

In the thermogram of collagen, there was a major peak in the range of 0−120 °C. The temperature corresponding to the structural change of lyophilized collagen was 68.1 °C [Figure 5A(c)]. In solution (5 mM acetic acid), collagen underwent a

Table 4. Thermal Parameters in Solid and Liquid States[a]

	lyophilized samples		samples in solution	
material	T (°C)	ΔH (J/g)	T (°C)	ΔH (J/g)
PVP	65.7	162.1	86.7	1295.0
PVPirr	74.5	126.9	92.5	1243.0
collagen	68.1	181.8	84.2	1723.0
C+PVP	54.2	242.0	84.2	1350.0
C−PVP	67.3	198.9	111.9	1489.0
C−PVP/−PVP	44.1	402.1	112.8	1614.0

[a]ΔH = enthalpy change.

pronounced change in the slope of the endothermic event at 39.9 °C, indicating the starting point of denaturation [Figure 5B(c)]. It was related to a conformational change in the structure of the triple helix, wherein destabilization occurred mainly due to disruption of intra- and intermolecular hydrogen bonds and due to retained water.[37]

For lyophilized C+PVP, the onset of the thermal transition was at 54.19 °C [Figure 5A(d)], indicating a shift to the left compared to that of collagen or PVP. The decrease in energy required to move the chains of the PVP polymer can be explained by the presence of collagen structure between the polymer chains, unlike the energy required for a pure sample of PVP. In solution, C+PVP also showed a leftward displacement compared to PVP, with a transition at 84.3 °C [Figure 5B(d)]. This shift was due to potential intermolecular hydrogen bonds formed between the collagen solution and PVP.[37]

A significant shift to the left was observed for lyophilized C−PVP/−PVP, with a temperature of 44.14 °C [Figure 5A(f)]. A higher value of ΔH (402.1 J/g) was also observed, indicating the presence of a new structure. This structural change was associated with T_g combined with the loss of water, where the new material had a lower heat resistance than collagen or PVP.

dx.doi.org/10.1021/jp502476x | J. Phys. Chem. B 2014, 118, 9272−9283

In contrast, C−PVP/−PVP in solution [Figure 5B(f)] had a higher heat resistance, with a high transition temperature (111.92 °C) due to the breaking of intramolecular hydrogen bonds and hydrogen bonding with water. Thus, the structural conformation of C−PVP/−PVP was more resistant to heat when in solution compared to that for collagen.

Lyophilized C−PVP showed a T_g of 67.31 °C [Figure 5A(e)], which markedly differed from the temperatures for C−PVP/−PVP and C+PVP. There was also a change in the values of ΔH. This difference in thermal behavior can be attributed to the presence of the residual fraction of PVP. Nevertheless, the effect was not evident when testing in solution.

Biochemical Susceptibility. Fibrillar collagens, such as type I collagen, are degraded in vivo by a well-defined group of MMPs, including MMP-1. To test whether the copolymer C−PVP was susceptible to digestion by the enzyme that normally breaks collagen, C−PVP was exposed to the enzyme for various time periods. C−PVP was almost immediately digested by MMP-1, as indicated by PAGE analysis. The banding pattern for C−PVP was similar to that of the type I collagen (Figure 6).

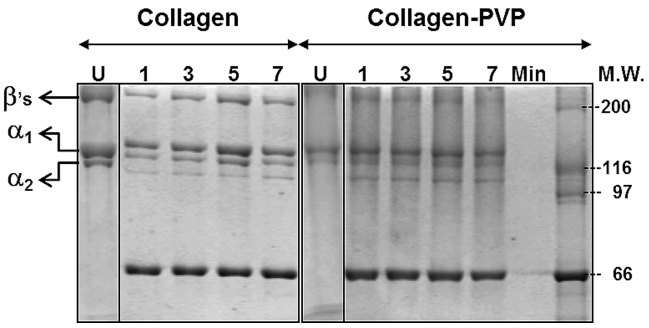

Figure 6. Images of polyacrylamide gels under denaturing conditions. Banding patterns of collagen and C+PVP, highlighting a fragment of approximately 70 kDa corresponding to that expected of three-fourths of the α chains derived from digestion by MMP-1. Lines marked "U" represent the protein or copolymer undigested; the numbers above the lanes represent incubation times in minutes. The bands corresponding to the type I collagen β and α chains are indicated on the left, and the molecular weight marker is indicated on the right.

This result indicates that the copolymer undergoes rapid hydrolysis in biological conditions by the same enzyme that digests endogenous collagen. The digested C−PVP fragment was slightly heavier than the corresponding collagen (Figure 6). This finding correlates with earlier results regarding the formation of the collagen and PVP copolymer.[16]

Rheology and Frequency Spectral Analysis. Rheology study was performed to determine the fluidic macroscopic properties of collagen and copolymers thereof because branches and/or cross-links strongly affect the dynamic properties of the polymers and copolymers. From the rheological study of the shear rate, it can be concluded that the copolymer and its collagen components are non-Newtonian fluids because the viscosity varied with shear rate and time. According to the profiles in Figure 7 (internal graphics), all of the materials assessed are pseudoplastic fluids whenever the absolute viscosity decreased with an increase of shear rate and $n < 1$. Table 5 shows the rheological parameters obtained from Ostwald's potential model with confidence intervals over 98%,[44,45] where irregularities and anomalies were evidenced when this model was performed. Therefore, other models were applied, such Williamson's model for pseudoplastics, Bingham's model for ideal plastics, and the model for the real plastic. However, unsatisfactory parameters were obtained in all cases. An analysis with the Herschel−Burkley model, which also did not fit our data, indicated that the irradiated compositions had a slight tendency toward behaving like Bingham's plastics. Namely, their consistency indices were the lowest, and their fluid characteristics were the highest.

One of the irregularities in the pseudoplastic behavior adjusted with the power law was that the C+PVP consistency was higher compared to that of the irradiated samples. This finding does not coincide with the experimental observations (Table 5). Still, it was considered that the samples behave as pseudoplastic fluids with a rheopectic character, given that the shear stress increased with the shear rate (Figure 7, external graphics) and with viscosity over time[46] (Figure 8). The collagen and C−PVP/−PVP samples (Figure 7a,c), which had a similar magnitude of viscosity that was greater than that of C+PVP or C−PVP (Figure 7b,d), exhibited an opposite separation profile, confirming the rheopectic behavior. There was a hysteresis loop at 6533.32 s^{-1} for collagen and 6933.33 s^{-1} for C−PVP/−PVP, which means that there wa a delay between the strain and stress (Figure 7). Specimens of C+PVP and C−PVP (Figure 7b,d) showed a smaller viscosity magnitude, with equivalent dynamics of their structural arrangements but without a defined hysteresis loop.

Clearly, excess PVP caused a decrease in viscosity (Figures 7 and 8). Given the shape of the profiles, it seems that the collagen governed the conformational structure of the copolymer. Possibly, the acidic pH of the PVP solution (pH 4.3) favored electrostatic interactions between PVP and collagen molecules, stabilizing the conformational structure during (variable or constant) shearing.

Next, the rate of change of the stiffness modulus was analyzed, calculated using the PWVD time−frequency spectra (Figure 9), in which the input signal was the strain derivative regarding the shear rate (σ) (for the variable shear experiment, an experimentalal time of t_E = 1950 s was employed, with N = 97 and $\Delta t_E = t_E/(N - 1) + 30 = 20.1$ s). All samples have the highest rates of change of the shear modulus around the boundary between the shear rate increasing and decreasing; these peaks correspond to the alignment of the molecules in the flow direction except at the value where the relaxation begins; in that, the bonds between the structures are strained. When the shear rate was increasing, the rate of change of the stiffness modulus was less marked in collagen and C−PVP (profiles, Figure 9a,d), whereas in C−PVP/−PVP, it progressively increased (profile, Figure 9c). In C+PVP, the rate of change appeared as a sharp Gaussian, with the peak amplitude at 4400 s^{-1} (profile, Figure 9b). Solutions of LMW PVP do not form stable structures;[47] therefore, the high rate of change of the stiffness modulus of C+PVP during increasing shear rate could be due to the structural mobility of PVP. This effect was seen when residual PVP was eliminated from the copolymer during decreasing shear rate (Figure 9c).

The maxima in the contour lines of the frequencies in Figure 9 (in 3D) indicate the major rates of change in the stiffness modulus. These results relate to the possible alignment of the polymer chains during increasing shear rate and with their restructuring or rearrangement during decreasing shear rate. The shape of the slopes, in the context of the extent and intensity of the contours along frequencies, suggested that after ordering its chains with the flow, C−PVP/−PVP (3D, Figure 9c) harmonically modify its stiffness modulus. In contrast, after

dx.doi.org/10.1021/jp502476x | J. Phys. Chem. B 2014, 118, 9272−9283

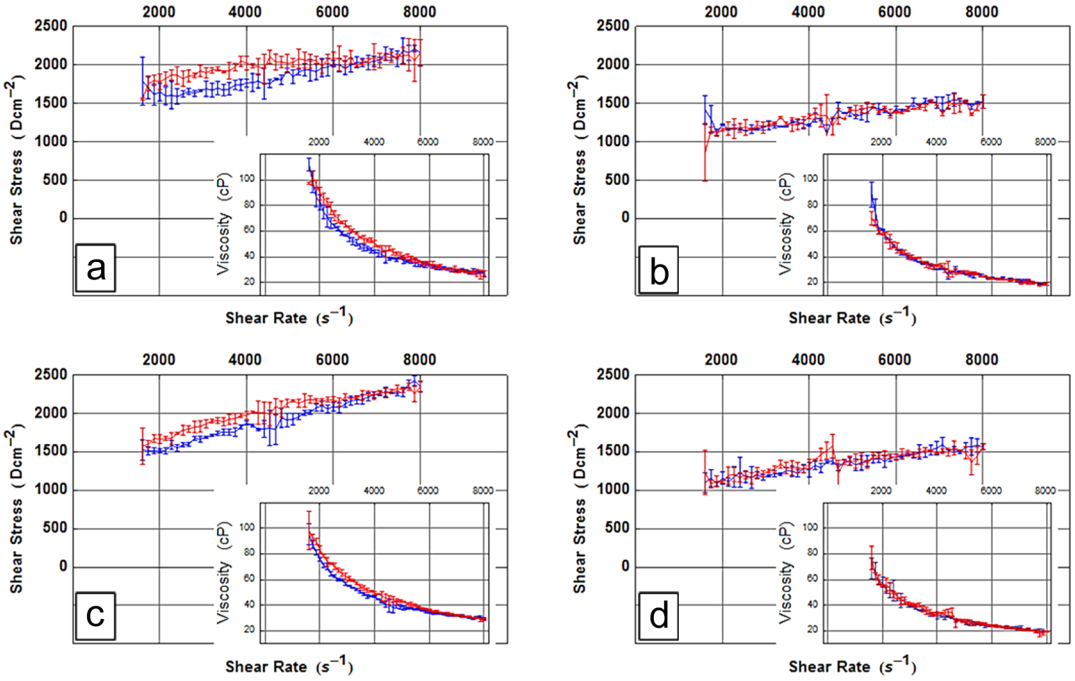

Figure 7. Variation of viscosity (inner graphs) and shear stress with applied shear rate for (a) collagen, (b) C+PVP, (c) C−PVP/−PVP, and (d) C−PVP. Increasing shear rate (blue line) and decreasing shear rate (red line). Data are means ± SDs of $N = 3$.

Table 5. Rheological Parameters by the Power Model[a]

sample	k	standard error k	n	standard error n	r^2
collagen	320.927	37.770	0.209	0.014	0.987
C−PVP/−PVP	131.180	11.999	0.319	0.011	0.991
C+PVP	267.382	45.708	0.192	0.020	0.987
C−PVP	172.611	14.399	0.244	0.098	0.987

[a]Consistency index (k) and fluid characteristic (n) (Newtonian = 1).

collagen (3D, Figure 9a) aligned its chains, the stiffness varies slightly asymptotically with the frequency. These findings suggest that C−PVP/−PVP is more mobile in its structural units than collagen. C+PVP, in contrast, significantly modifies its fluency variation, especially at 4400 s^{-1}, for all frequencies, whereas C−PVP (3D, Figure 9d) showed weak structural changes with frequency after ordering its chains with increasing shear rate.

With respect to the behavior during decreasing versus increasing shear rate, C−PVP/−PVP had the greatest symmetry in its profiles, compared to collagen (profiles and

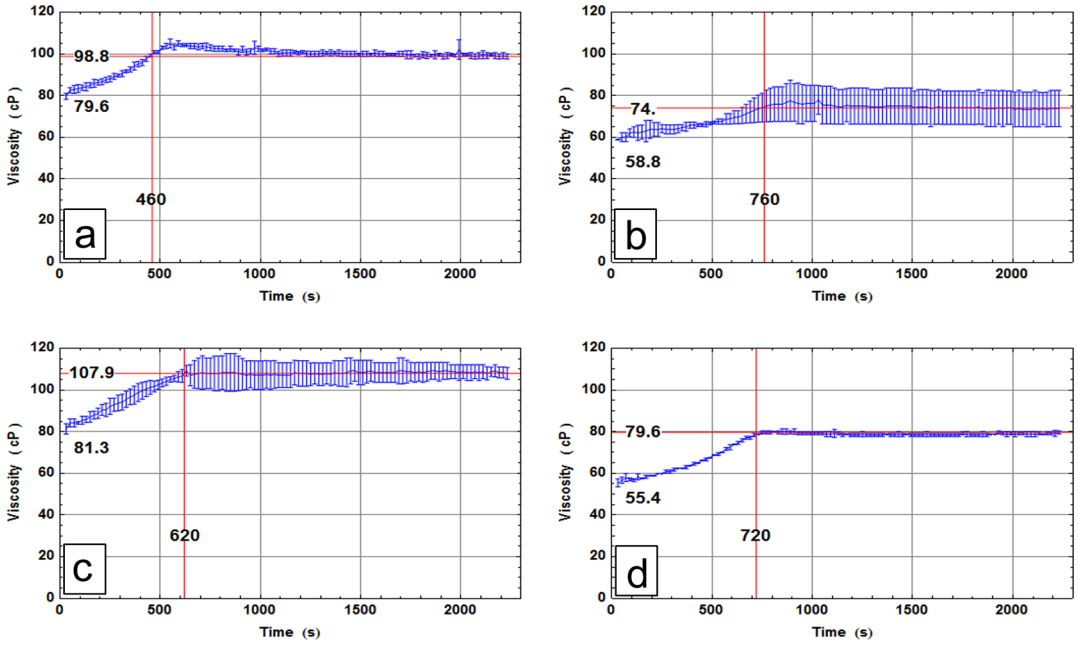

Figure 8. Variation of the viscosity across time for (a) collagen, (b) C+PVP, (c) C−PVP/−PVP, and (d) C−PVP. Data are means ± SDs of $N = 3$.

dx.doi.org/10.1021/jp502476x | J. Phys. Chem. B 2014, 118, 9272−9283

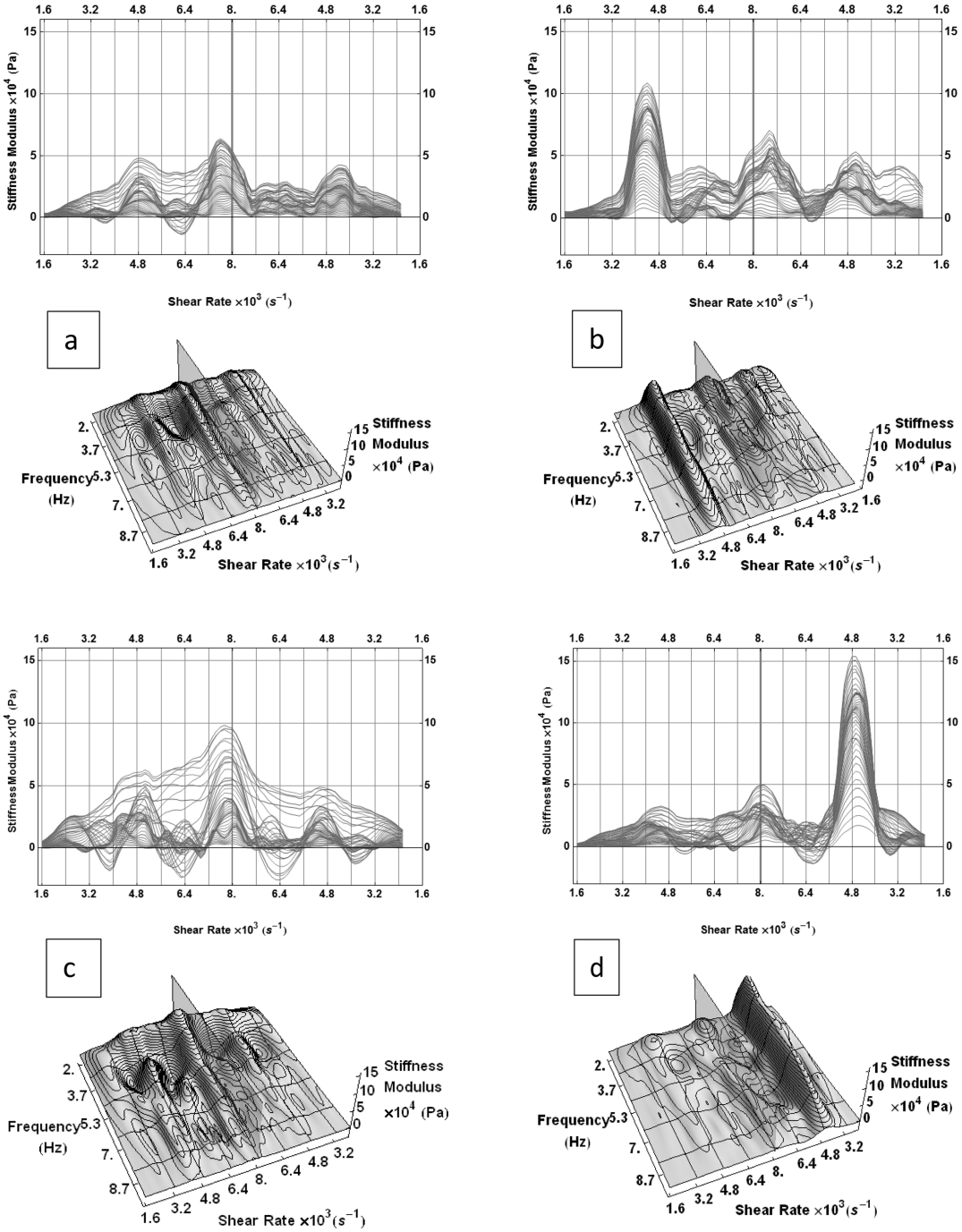

Figure 9. PWVD of variable shear rate rheograms. The upper panels show frequency profiles projected in the plane of the shear rate and the stiffness modulus. 3D graphs correspond to the spectral densities of frequencies. Thick lines correspond to regions of increasing shear rate. Translucent planes correspond to regions with decreasing shear rate. $N = 96$, $t = 20.1$ s, smoothed window size = 4 × 4. (a) Collagen, (b) C+PVP, (c) C−PVP/−PVP, and (d) C−PVP.

Figure 9c,a). This result implies a relaxation dynamics closer to that of the ideal plastic but with more consistency. The irregular shape of the front of the contours indicates that C−PVP/−PVP had a more fluid behavior than collagen (3D, Figure 9c,a, respectively), as predicted by the power law (Table 5). C+PVP relaxed in an irregular manner, with considerable variation in its structural arrangements (3D, Figure 9b). C−PVP showed a high and sustained rate of its fluency variation during the relaxation, in 4670 s^{-1} for all frequencies (3D, Figure 9d). The irregular shape of the front edges of the contour and its frequency extension suggest that C+PVP was more fluid than the other samples.

Interaction with the $\alpha_2\beta_1$ Receptor and Biochemical Activity. The biological phenomenon of contraction can be reproduced in a 3D model in vitro, wherein the effect depends on the interaction of the cells through their membrane receptors and the ECM. Therefore, it was considered that if C−PVP retains some of the physicochemical properties of native collagen, then it is possible that its interaction with cells (fibroblasts) could occur through the collagen receptors. In particular, the heterodimer formed by the $\alpha_2\beta_1$ integrin was

dx.doi.org/10.1021/jp502476x | J. Phys. Chem. B 2014, 118, 9272−9283

considered, which is a classical type I collagen receptor in animal tissues. When 3D cultures of human fibroblasts were treated with various concentrations of copolymer, we observed no contraction by the application of C−PVP to the system, regardless of whether the copolymer was added before or after the polymerization of the gel formed by collagen in the culture (Figure 10a). However, application of C−PVP did cause changes in the expressions of the integrin α_2 chain (Figure 10b) and prolyl hydroxylase (Figure 10c). Thus, although the biological effect of the copolymer is not generated from its interaction with the receptor selected in this work, it does produce changes in the collagen metabolism as well as in the expression of ECM receptors.

DISCUSSION

The C−PVP copolymer is a biosynthetic hybrid formed by one of the most abundant proteins in the animal kingdom (collagen) and a LMW polymer (PVP). Physicochemical properties of PVP allow it to be highly soluble in hydrophilic and hydrophobic media, besides that it has multiple applications in different technological fields, ranging from industry to health. The structure of C−PVP maintained part of the collagen properties, combined with the film-forming properties of PVP, with the exception that cross-linking through γ irradiation partially fragmented the copolymer, probably without denaturation.

NMR analysis provides structural evidence; meanwhile, SEM analysis demonstrates morphological characteristics; in this work, the results derived from the analysis of the copolymer using both techniques were consistent, revealing that the molecular changes induced by cross-linking collagen with PVP are evident. Stoichiometrically, 55.8% of the C−PVP copolymer was PVP polymerized with type I collagen; thus, the free fraction could have an important role in protecting the protein component from radiation. When collagen alone or collagen with smaller proportions of free PVP was irradiated, a highly cross-linked solid gel was formed (unpublished observations). When free PVP was removed (C−PVP/−PVP), the irradiated copolymer exhibited fundamental changes in its structure; its disarrangement was slower than its rearrangement after being subjected to shear stress (Figure 7). This effect was due to the collagenous component, whose structural domain was clear and distinguishable from the free polymer aggregates of PVP (Figure 3B). Collagen−PVP/−PVP maintained the same rheological properties as the pharmaceutical copolymer (C−PVP), with a non-Newtonian and pseudoplastic behavior, with the particularity that the pure form without excess PVP tended toward plasticity. These results that do not smatch with the Ostwald model were due to the fact that the irradiated compositions of collagen and PVP lost their pseudoplastic character and became slightly plasticized, which allowed them to deform without losing too much energy with increasing stress on them. Possibly, the high production of free radicals during the irradiation process favors the formation of covalent bonds between PVP and collagen; this feature combined with the idea that the lattice structure of the copolymer is broken down into smaller fragments[37] may explain why C−PVP manifested small variations in the shear modulus with increasing shearing rates, why C−PVP/−PVP was more mobile than PVP, and why the shear modulus of C+PVP exhibited such great variability. Given the microscopically observed film morphology, we propose that the 3D network of long chains of C−PVP retains the solvent water through

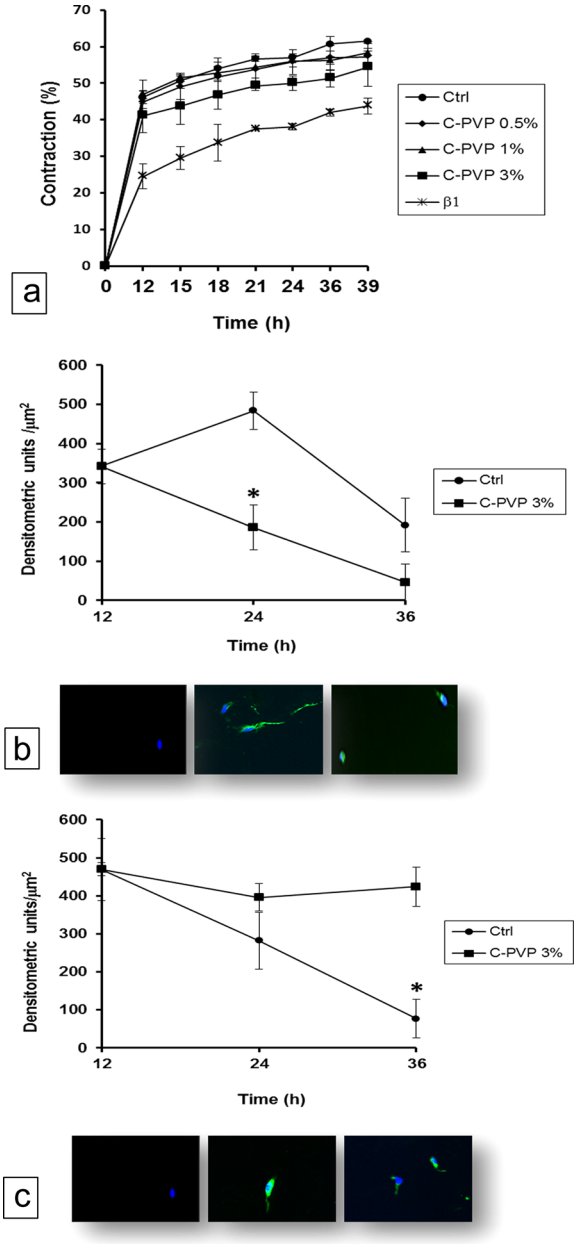

Figure 10. Biological effects of C−PVP in a 3D model of fibroblasts. (a) Rate of contraction. No statistically significant differences were found between untreated control cultures and cultures treated with different concentrations (%) of copolymer. Positive control, which was treated with an antibody against the integrin β1 subunit, showed a delay in the contraction (β1 in chart); bars represent the standard deviation. (b) Kinetics of the expression experiments during treatment with 3% of C−PVP; (b) α_2 subunit and (c) prolyl hydroxylase. Bars represent the standard error of the mean. The statistically significant difference between the control and treatment is represented by *; p = 0.016 and $p < 0.001$ (in a and b, respectively). Photomicrographs below the chart show representative images of (from left to right) the blank, control cultures, and cultures treated with 3% of the copolymer at the 24 h point. Nuclei are stained blue (DAPI), and the antigens, α_2 subunit, or prolyl hydroxylase are stained green (FITC).

hydrophilic groups, a property that, in pseudoplastic fluids, results in a deviation in behavior toward that characteristic of Bingham's ideal plastic. This result can be related to the evidence that C−PVP demonstrates different properties from those of its components. When we considered the dynamic

dx.doi.org/10.1021/jp502476x | J. Phys. Chem. B 2014, 118, 9272−9283

properties of the compound in bulk (C+PVP), we discovered significant differences from the copolymer. As solutions of LMW PVP do not form stable structures,[47] the high rate of the shear modulus change of C+PVP during increasing shear rate was due to the structural mobility of PVP. This effect was observed when disaggregating the copolymer (C−PVP) from the residual PVP during decreasing shear rate (Figure 7c,d).

The functional interaction of the copolymer with cells was assessed via a competitive assay in vitro, which sought the inhibitory effect of C−PVP upon contraction of the ECM. The copolymer had biological effects on the expressions of integrin α_2 and prolyl hydroxylase. However, its interaction with the cells was not through the collagen receptors as the copolymer did not inhibit or slow the effect of contraction. Therefore, we consider that C−PVP might exert its pharmacological effect through other means, at least in fibroblasts. Specifically, the effect may occur through one or more of its metabolites generated by the effects of MMPs, such as MMP-1.

CONCLUSIONS

As a result of these structural characteristics, the copolymer exhibited the following properties in solution when compared to "native" collagen: (1) agglomerates with smaller size, (2) increased resistance to thermal shock, (3) lower speed and fluidity under a constant progressive stress, and (4) similar susceptibility to enzymatic digestion by MMP-1 but different metabolic activity.

AUTHOR INFORMATION

Corresponding Author

*E-mail: kroted@yahoo.com.mx. Tel.: +52(55) 5999 1188. Address: Laboratory of Connective Tissue, Centro Nacional de Investigación y Atención de Quemados, Instituto Nacional de Rehabilitación. Calzada México-Xochimilco No. 289, Colonia Arenal de Guadalupe, Delegación Tlalpan, 14389 Mexico City, Mexico.

Notes

The authors declare no competing financial interest.

ACKNOWLEDGMENTS

The authors thank Carlos Flores for AFM assessment, Omar Novelo for SEM assays, Gerardo Cedillo for NMR-MAS analysis, Blanca Graciela Medina Vara for participating in physicochemical assays, Aspid SA de CV for the donation of C−PVP and its source materials, and Kate Edmondson from Write Science Right for English translation and editorial review.

REFERENCES

(1) Chimal-Monroy, J.; Bravo-Ruíz, T.; Furuzawa-Carballeda, G. J.; Lira, J. M.; de la Cruz, J. C.; Almazán, A.; Krötzsch-Gómez, F. E.; Arrellín, G.; Díaz de León, L. Collagen-PVP Accelerates New Bone Formation of Experimentally Induced Bone Defect in Rat Skull and Promotes the Expression of Osteopontin and SPARC during Bone Repair of Rat Femora Fractures. *Ann. N.Y. Acad. Sci.* **1998**, *857*, 232−236.

(2) Furuzawa-Carballeda, C.; García-Aranda, R.; Furuzawa-Carballeda, J. Estudio Piloto sobre la Eficacia del Uso de la Colágena-polivinilpirrolidona (clg-PVP) en la Regeneración Ósea en Cirugía Endodóncica. *Rev. Odontol. Mex.* **2005**, *9*, 191−196.

(3) Ascencio, D.; Hernández-Pando, R.; Barrios, J.; Soriano, R. E.; Perez-Guille, B.; Villegas, F.; et al. Experimental Induction of Heterotopic Bone in Abdominal Implants. *Wound Rep. Reg.* **2004**, *12*, 643−649.

(4) Cuéllar, E.; Mina, N. Jumper's Knee. Surgery and Arthroscopic Treatment with Scraping and Povidone Collagen in High-Performance Athletes. *Acta Ortop. Mex.* **2007**, *21*, 234−238.

(5) Padilla, L.; Krötzsch, E.; Schalch, P.; Figueroa, S.; Miranda, A.; Rojas, E.; Esperante, S.; Villegas, F.; de la Garza, A. S.; Di Silvio, M. Administration of Bone Marrow Cells into Surgically Induced Fibrocollagenous Tunnels Induces Angiogenesis in Ischemic Rat Hindlimb Model. *Microsurgery* **2003**, *23*, 568−574.

(6) Cervantes-Sánchez, C. R.; Olaya, E.; Testas, M.; Garcia-López, N.; Coste, G.; Arrellin, G.; Luna, A.; Krötzsch, F. E. Collagen−PVP, a Collagen Synthesis Modulador, Decreases Intraperitoneal Adhesions. *J. Surg. Res.* **2003**, *110*, 207−210.

(7) de Hoyos, A.; Monroy, M. A.; Checa, G.; Rodriguez, P. Collagen/Povidone as a New Endoscopic Treatment Option in Peptic Ulcer Bleeding. *Endoscopy* **2006**, *38*, 99.

(8) Dé Hoyos-Garza, A.; Aguilar, E.; Richards, G. Ileocolonic Ulcer Treated by Endoscopic Application of Collagen−Polyvinylpyrrolidone. *Can. J. Gastroenterol.* **2007**, *21*, 513−515.

(9) Furuzawa-Carballeda, J.; Krötzsch-Gómez, E.; Barile-Fabris, L.; Alcalá, M.; Espinosa-Morales, R. Subcutaneous Administration of Collagen−Polyvinylpyrrolidone Down Regulates IL-1b, TNF-a, TGF-b1, ELAM-1 and VCAM-1 Expression in Scleroderma Skin Lesions. *Clin. Exp. Dermatol.* **2005**, *30*, 83−86.

(10) Zerón, H. M.; Krötzsch-Gómez, F. E.; Muñoz, R. E. Presure Ulcers: A Pilot Study for Treatment with Collagen Polyvinylpyrrolidone. *Int. J. Dermatol.* **2007**, *46*, 314−317.

(11) Suárez-Colín, A.; Salgado, R. M.; Apis-Hernández, A. M.; Krötzsch-Gómez, E. Inducción del Tejido de Granulación por Pasta de Lassar vs. Colágena−Polivinilpirrolidona en Úlceras por Insuficiencia Venosa. *Cir. Plast.* **2004**, *14*, 5−13.

(12) Krötzsch, E.; Furuzawa-Carballeda, J.; Reyes-Márquez, R. Cytokine Expression is Down Regulated by Collagen−Polyviylpyrrolidone in Hypertrophic Scars. *J. Invest. Dermatol.* **1998**, *111*, 828−834.

(13) Furuzawa-Carballeda, J.; Cabral, A. R.; Zapata-Zuñiga, M.; Alcocer-Varela, J. Subcutaneous Administration of Polymerized-Type-I Collagen for the Treatment of Patients with Rheumatoid Arthritis. An Open-Label Pilot Trial. *J. Rheumatol.* **2003**, *30*, 256−259.

(14) Furuzawa-Carballeda, J.; Rodríguez-Calderón, R.; Diaz de León, L.; Alcocer-Varela, J. Mediators of Inflammation are Down-Regulated while Apoptosis is Up-Regulated in Rheumatoid Arthritis Synovial Tissue by Polymerized Collagen. *Clin. Exp. Immunol.* **2002**, *130*, 140−149.

(15) Furuzawa-Carballeda, J.; Muñoz-Chablé, O. A.; Barrios-Payán, J.; Hernández-Pando, R. Effect of Polymerized-Type I Collagen in Knee Osteoarthritis. I. In Vitro Study. *Eur. J. Clin. Invest.* **2009**, *39*, 591−597.

(16) Chimal-Monroy, J.; Bravo-Ruiz, T.; Krötzsch-Gómez, E.; Diaz de León, L. Implantes de Fibroquel aceleran la formación de hueso nuevo en defectos óseos inducidos experimentalmente en cráneos de rata: un estudio histológico. *Rev. Biomed.* **1997**, *8*, 81−8.

(17) Krotzsch-Gómez, F. E.; Diaz de Leon, L. Effect of FibroquelMR on Collagen Metabolism in Cellular Cultures. *Wound Rep. Reg.* **1995**, *3*, 95.

(18) Furuzawa-Carballeda, J.; Rojas, E.; Valverde, M.; Diaz de León, L.; Krötzsch, E. Cellular and Humoral Responses to Collagen−Polyvinylpyrrolidone Administered during Short and Long Periods in Humans. *Can. J. Physiol. Pharmacol.* **2003**, *81*, 1029−1035.

(19) Sionkowska, A.; Skopinska, J.; Wisniewski, M. Photochemical Stability of Collagen/poly(vinyl alcohol) Blends. *Polym. Degrad. Stab.* **2004**, *83*, 117−125.

(20) Rochdi, A.; Foucat, L.; Renou, J. NMR and DSC Studies during Thermal Denaturation of Collagen. *Food Chem.* **2000**, *69*, 295−299.

(21) Piñón-Segundo, E.; Ganem-Quintanar, A.; Alonso-Pérez, V.; Quintanar-Guerrero, D. Preparation and Characterization of Triclosan Nanoparticles for Periodontal Treatment. *Int. J. Pharm.* **2005**, *294*, 217−32.

(22) Cerofolini, L.; Fields, G. B.; Fragai, M.; Geraldes, C. F.; Luchinat, C.; Parigi, G.; Ravera, E.; Svergun, D. I.; Teixeira, J. M. Examination of Matrix Metalloproteinase-1 in Solution: A Preference

for the Pre-collagenolysis State. *J. Biol. Chem.* **2013**, *288*, 30659−30671.
(23) Ville, J. Theorie et Application de la Notion de Signal Analytical. *Cables Transm.* **1948**, *2a*, 61−74.
(24) Shin, Y.; Jeon, J. Pseudo Wigner−Ville Time−Frequency Distribution and Its Application to Machinery Condition Monitoring. *Shock Vib.* **1993**, *1*, 65−76.
(25) Wahl, T. J.; Bolton, J. S. The Application of the Wigner Distribution to the Identification of Structure-Borne Noise Components. *J. Sound Vib.* **1993**, *163*, 101−122.
(26) Eckes, B.; Mauch, C.; Hüppe, G.; Krieg, T. Downregulation of Collagen Synthesis in Fibroblasts within Three-Dimensional Collagen Lattices Involves Transcriptional and Posttranscriptional Mechanisms. *FEBS Lett.* **1993**, *318*, 129−33.
(27) Mauch, C.; Hatamochi, A.; Scharffetter, S.; Krieg, T. Regulation of Collagen Synthesis in Fibroblasts within a Three-Dimensional Collagen Gel. *Exp. Cell. Res.* **1988**, *178*, 493−503.
(28) Delvoye, P.; Nusgens, B.; Lapiere, C. M. The Capacity of Retracting a Collagen Matrix Is Lost by Dermatosparactic Skin Fibroblasts. *J. Invest. Dermatol.* **1983**, *81*, 267−270.
(29) Sionkowska, A.; Planecka, A.; Kozlowska, J.; Skopinska-Wisniewska, J. Collagen Fibrils Formation in Poly(vinyl alcohol) and Poly(vinyl pyrrolidone) Films. *J. Mol. Liq.* **2009**, *144*, 71−74.
(30) Gelse, K.; Pöschl, E.; Aigner, T. Collagens—Structure, Function, and Biosynthesis. *Adv. Drug Delivery Rev.* **2003**, *55*, 1531−1546.
(31) Sionkowska, A.; Wisniewski, M.; Kaczmarek, H.; Skopinska, J.; Chevallier, P.; Mantovani, D.; Lazarec, S.; Tokarevc, V. The Influence of UV Irradiation on Surface Composition of Collagen/PVP Blended Films. *Appl. Surf. Sci.* **2006**, *253*, 1970−1977.
(32) Dumitraşcu, M.; Albu, M. G.; Vîrgolici, M.; Vancea, C.; Meltzer, V. Characterization of Electron Beam Irradiated Polyvinylpyrrolidone−Dextran (PVP/DEX) Blends. *Solid State Phenom.* **2012**, *188*, 102−108.
(33) Kalinowski, H. O.; Berger, S.; Braun, S. *Carbon-13 NMR Spectroscopy*; John Wiley & Sons: New York, 1988.
(34) Mayo, K. H. NMR and X-ray Studies of Collagen Model Peptides. *Biopolymers.* **1996**, *40*, 359−370.
(35) Wüthrich, K. NMR Studies of Structure and Function of Biological Macromolecules. *Angew. Chem. Int.* **2003**, *42*, 3340−3363.
(36) Wider, G. Technical Aspects of NMR Spectroscopy with Biological Macromolecules and Studies of Hydratation in Solution. *Prog. Nucl. Magn. Reson. Spectrosc.* **1998**, *32*, 193−275.
(37) Sionkowska, A. Interaction of Collagen and Poly(vinyl pyrrolidone) in Blends. *Eur. Polym. J.* **2003**, *39*, 2135−2140.
(38) Leikina, E.; Mertts, M.; Kuznetsova, N.; Leikin, S. Type I Collagen Is Thermally Unstable at Body Temperature. *Proc. Natl. Acad. Sci. U.S.A.* **2002**, *99*, 1314−1318.
(39) Zerrouk, N.; Mennini, N.; Maestrelli, F.; Chemtob, C.; Mura, P. Comparison of the Effect of Chitosan and Polyvinylpyrrolidone on Dissolution Properties and Analgesic Effect of Naproxen. *Eur. J. Pharm. Biopharm.* **2004**, *57*, 93−99.
(40) Abdelkader, H.; Abdallah, O. Y.; Salem, H. S. Formulation of Controlled-Release Baclofen Matrix Tablets: Influence of Some Hydrophilic Polymers on the Release Rate and In Vitro Evaluation. *AAPS Pharm. Sci. Technol.* **2007**, *8*, 156−166.
(41) Kalogeras, I. M. A Novel Approach for Analyzing Glass-Transition Temperature vs. Composition Patterns: Application to Pharmaceutical Compound + Polymer Systems. *Eur. J. Pharm. Sci.* **2011**, *42*, 470−483.
(42) Fitzpatrick, S.; McCabe, J. F.; Petts, C. R.; Booth, S. W. Effect of Moisture on Polyvinylpyrrolidone in Accelerated Stability Testing. *Int. J. Pharm.* **2002**, *246*, 143−151.
(43) Freudenberg, U.; Behrens, S. H.; Welzel, P. B.; Müller, M.; Grimmer, M.; Salchert, K.; Taeger, T.; Schmidt, K.; Pompe, W.; Werner, C. Electrostatic Interactions Modulate the Conformation of Collagen I. *Biophys. J.* **2007**, *92*, 2108−2119.
(44) Sulea, D.; Ghica, M. V.; Micutz, M.; Albu, M. G.; Brazdaru, L.; Staicu, T.; Leca, M.; Popa, L. Characterization and In Vitro Release of Chlorhexidine Digluconate Comprised in Type I Collagen Hydrogels. *Rev. Roum. Chim.* **2010**, *55*, 543−551.
(45) Kahn, L. D.; Witnauer, L. P. The Viscometric Behavior of Solubilized Calf Skin Collagen at low Rates of Shear. *J. Biol. Chem.* **1966**, *241*, 1784−1789.
(46) Oates, K. M.; Krause, W. E.; Jones, R. L.; Colby, R. H. Rheopexy of Synovial Fluid and Protein Aggregation. *J. R. Soc., Interface* **2006**, *3*, 167−174.
(47) Mayo-Pedrosa, M. *Pellets Sensibles a Estímulos para Liberación Controlada de Medicamentos: Reticulación de Matrices y Formación de Cubiertas In Situ*, Ph.D. Thesis. Universidad de Santiago de Compostela, Santiago de Compostela, España, 2008.

NOTE ADDED AFTER ASAP PUBLICATION

This paper was published ASAP on July 30, 2014. The abstract graphic was updated. The revised paper was reposted on August 7, 2014.